IIETA International Information and Engineering Technology Association
Advancing the World of Information and Engineering

Traitement du Signal
Vol. 39, No. 5, October, 2022, pp. 1597-1603
Journal homepage: http://iieta.org/journals/ts

Image Segmentation and Target Extraction of Preschool Educational Activity Space for Improving Children's Concentration

Ting Jin[1], Zhuang Ma[1], Jinfang Niu[1], Peng Su[2*]

[1] Education Scientific College, Henan Finance University, Zhengzhou 450046, China
[2] Jitang College, North China University of Science and Technology, Tangshan 063210, China

Corresponding Author Email: Supeng@ncst.edu.cn

https://doi.org/10.18280/ts.390516

Received: 3 June 2022
Accepted: 7 September 2022

Keywords:
children's concentration, preschool education, activity space, image segmentation, object extraction

ABSTRACT

Concentration is crucial for children to nurture good personality and develop well. To observe teachers and children in concentration-oriented preschool education activities, it is necessary to analyze the video images of relevant activities. This paper the image segmentation and target extraction of preschool education activity space for improving children's concentration. After discussing the relationship between children's concentration and preschool educational activity intervention, the authors introduced the frequency-tuned saliency algorithm into the constructed Gaussian mixture model, constructed the spatial information of the images on the preschool educational activity space for improving children's concentration, and successfully segmented these images. Since the target children are small and numerous, have color overlap with the background, and face strong light interference, the ViBe algorithm with complex scenes, i.e., ViBe+, was selected to quickly detect the multiple child targets in complex preschool education activity environments. Experimental results verify the effectiveness of the proposed algorithm.

1. INTRODUCTION

Children's pointing and concentrate on specific things are examples of children's psychological activity, and these actions are referred to as children's concentration [1, 2]. Children's mental activity are said to be direct when they point away from one thing at a specific point and toward other objects, a sign of their selectivity [3-6]. Although it cannot be compared to a child's IQ, a child's intelligence will be somewhat impacted by their level of concentration. It might be stated that children's character development and excellent character formation depend on their ability to concentrate [7-9].

The majority of the time, teachers will carry out preschool education activities based on the user's needs for concentration training, such as clapping games, operational activities, mirror games, and other enjoyable activities, or group dances, aerobics, cheerleading, stacking arhats, rubber band jumping, archery, and other sports activities, or develop independent activity plans in accordance with student individual differences [10-18]. It is necessary to analyze relevant activity video images to support the follow-up teachers in sorting out the principles and strategies for observing and analyzing children's behaviors in activities in order to achieve effective observation of teachers and children in preschool education activities intended to cultivate children's concentration.

Children find it challenging to focus while learning online. Facial expressions are crucial for grabbing pupils' attention in the present, according to Yu and Luo [19]. The researchers build a student attention prediction model using the self-healing network (SCN) method and the random forest method based on C4.5 based on the facial expression data of students and the attention scores provided by teachers in online teaching activities in an elementary school. This model is then used in actual online teaching. Kokkalia et al. [20] investigated play that supported toddlers with cognitive, intellectual, physical, and literacy challenges. It also investigated how instructional video games can benefit brilliant youngsters and children with developmental disabilities like autism. Through the use of a smart watch device, Hosseini et al. [21] investigated the issue of recognizing children's activity. Bidirectional LSTM model and fully connected deep network are the two deep neural network models that are used, and the outcomes are contrasted with other models that are frequently employed in the field. In comparison to the baseline model, experimental results show that the proposed deep model can greatly improve the results. It also highlights the benefit of activity intensity level identification in health monitoring and confirms the suggested model's excellent performance in this task. Particularly for toddlers and young children, the current system does not account for all age ranges. To obtain benchmark results for various unimodal and multimodal settings, Basak et al. [22] compares the performance of currently available tools and algorithms. Children's faces are the simplest modality to record, according to the data, which also demonstrate great verification performance.

Video surveillance, human-computer interaction, television and movies, the military, and sports are just a few of the many industries where segmentation and extraction of moving objects for dynamic scenarios are used. According to a survey of the literature, the majority of studies in the aforementioned applied research topics focus on object tracking, event monitoring, video content retrieval, and object categorization. Comparatively few studies have focused specifically on the examination of photographs of children's activity spaces. For the purpose of cultivating children's concentration, this study

performs research on the image segmentation and target extraction of preschool education activity space. The relationship between preschool educational activities and children's concentration is discussed in Section 2, and the frequency-tuned salience algorithm is introduced into the Gaussian mixture model created to realize the spatial images of preschool educational activities for the development of children's concentration, creation of spatial information and active segmentation of spatial images. In Section 3, the ViBe algorithm ViBe+ of complex scenes is chosen to realize the target recognition of multiple children in a complex preschool educational environment. This algorithm is targeted at issues like small target children, large numbers of target children, overlap of target children and background colors, or strong light interference, etc. The efficiency of the algorithm is confirmed by experimental data.

2. IMAGE SEGMENTATION

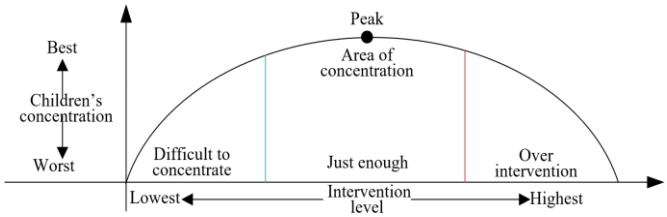

Figure 1. Curve between children's concentration and preschool education intervention

Figure 1 depicts an inverted U-shaped link between preschool educational activity intervention and children's attention span. Children's concentration will improve with an increase in preschool education activity intervention within a specified range. Children's concentration will decline as the amount of preschool education activity intervention increases once it goes beyond a certain range. That is to say, preschool education activities' degree of intervention is too low to effectively affect children's concentration, and if the activities are excessively intervened, it would have a negative influence on the children's concentration. As a result, the development of children's concentration is greatly influenced by the appropriate intervention intensity of preschool education activities, i.e., the reasonable activity or sports form and activity intensity of preschool education activities, and teachers or other scholars urgently need to conduct in-depth research.

This paper analyzes the relevant activity video images to provide theoretical reference and technology for teachers to observe and analyze the principles and strategies of children's behavior in activity support, in order to achieve effective observation of teachers and children in preschool education activities aimed at cultivating children's concentration. The correlation of pixel space in the target children's region must be taken into account in the spatial image processing of preschool education activities for the cultivation of children's concentration. The lack of continuity in the pixel segmentation process, the addition of spatial information, the easy loss of edge information, complex solutions, and time-consuming calculations are only a few of the issues with current image processing techniques. In light of the aforementioned issues, this research implements the building of the spatial information of the preschool educational activity spatial image and incorporates the frequency tuning saliency method into the developed image processing model.

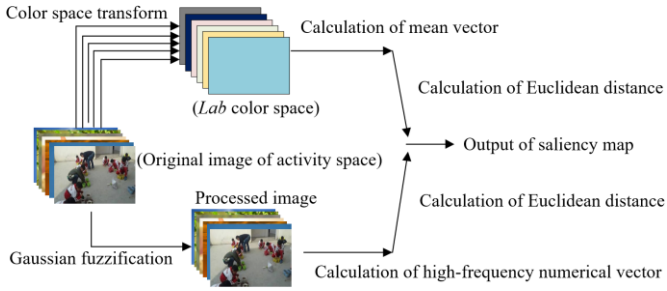

Figure 2. Flow of saliency extraction

The preschool education activity space image's low-frequency and high-frequency bands, respectively, correlate to the general information and specific information of the target children in the image. The approach removes the highest frequency information from the image of the preschool education activity space by smoothing the noise using a 5×5 Gaussian window. The extraction process of spatial image saliency in preschool educational activities is depicted in Figure 2. Assuming that a_i represents the k-th pixel in the activity space image, RG_λ represents the mean feature vector of the activity space image in the Lab color feature space, $RG_{qfd(ai)}$ represents the corresponding activity space image pixel feature after the Gaussian blur operation, and $\|.\|$ represents the L_2 normal forms. Following are the formulas for determining the saliency map value of an activity space image pixel:

$$O(a_i) = \left\| RG_\lambda - RG_{qf_d}(a_i) \right\| \tag{1}$$

This paper is based on the Gaussian mixture model $GMM+$ which introduces frequency-tuned salience to realize the image segmentation and target extraction of the preschool education activity space images for the cultivation of children's concentration.

Assume that the i-th distribution function is represented by $E(a_i|\omega)$, the total number of labels of different types is represented by L, the i-th distribution function is represented by $E(a_i|\omega_l)$, and the weight of each function in the overall model is represented by κ_l. Then, the finite mixture model can be expressed as:

$$E(a_i \mid \omega) = \sum_{l=1}^{L} \kappa_l E(a_i \mid \omega_l) \tag{2}$$

Since the distribution of pixels in an activity space image of a dynamic scene is usually characterized by a Gaussian distribution. Suppose the gray value of the sample is represented by a, the average value of the sample is represented by λ, the covariance value of the Gaussian distribution is represented by $\sum$, the exponential function based on the natural number p is represented by $exp\{\cdot\}$, and the transposition of the vector is represented by R, and the input sample dimension is represented by Z. Then, the Gaussian distribution can be expressed as:

$$\Omega(a \mid \lambda, \Sigma) = \frac{1}{(2\kappa)^Z |\Sigma|^{\frac{1}{2}}} exp\left\{ -\frac{1}{2}(a-\lambda)^T \Sigma^{-1}(a-\lambda) \right\} \tag{3}$$

To unify and facilitate the processing of grayscale activity space images and RGB activity space images, the sample dimension is uniformly set to 2. Assume that the prior probability of pixel distribution, that is, the weight of the mixed components is expressed by $\Lambda=\{\kappa_1,\kappa_2,...,\kappa_K\}$, which satisfies $\sum_{j=1}^{K}\kappa_j=1$. Assume that the index value of the activity space image pixel is represented by i, and the index of the class label is represented by j, $i=\{1,2,...,M\}$, $j=\{1,2,...,K\}$, the mean and covariance of the j-th Gaussian distribution function are represented by $\omega_j=\{\lambda_j,\sum_j\}$. Let $\Psi=\{\omega_1,\omega_2,...,\omega_K\}$ satisfy $\omega_j=\{\lambda_j,\sum_j\}$. The set of parameters of the complete Gaussian distribution is denoted by Ψ. The total number of labels of different classes is represented by K. Then, the Gaussian mixture model can be expressed as:

$$E\left(a_i \mid \Lambda,\Psi\right)=\sum_{j=1}^{K}\kappa_j\Omega\left(a_i \mid \omega_j\right) \tag{4}$$

The Gaussian mixture model can divide the M pixels of the activity space image into L class labels, and introduce the spatial information reflected by the salient pixels of the active space image to the Gaussian mixture model by assigning appropriate weights. Assuming that the prior probability for the i-th pixel to be divided into the j-th class is represented by κ_{ij}, the j-th Gaussian distribution is represented by $E(a_n|\Psi_j)$, the neighborhood used to characterize a_i is represented by M_i, the index value of the pixel in neighborhood M_i of a_i is represented by n; the sum of saliency mapping values of all pixels in the neighborhood is denoted by T_i; the saliency mapping value of pixel a_n is denoted by $O(a_n)$, and all parameter sets involved in the model are denoted by Φ, satisfying $\Phi=\{\kappa_{11},\kappa_{12},...,\kappa_{1L},\kappa_{21},\kappa_{22},...,\kappa_{m1}\kappa_{m2},...,\kappa_{mk},\Psi_1,\Psi_2,...,\Psi_k\}$. The corresponding mathematical model can be expressed as:

$$g\left(a_i \mid \Phi\right)=\sum_{j=1}^{K}\kappa_{ij}\left[\sum_{n\in M_i}\frac{O\left(a_n\right)}{T_i}E\left(a_n \mid \omega_j\right)\right] \tag{5}$$

The *EM* algorithm is employed in this research to solve and optimize the model's parameters. The posterior probability, which gauges the likelihood of events connected to preschool education activities, is represented as α_{ij} under the assumption that W represents the objective function's logarithmic likelihood function. The complete data logarithmic likelihood function of the model's objective function can be given by:

$$W=\sum_{i=1}^{M}\sum_{j=1}^{K}\alpha_{ij}\left[\sum_{n\in M_i}\frac{O\left(a_n\right)}{T_i}\log E\left(a_n \mid \Psi_j\right)+log\kappa_{ij}\right] \tag{6}$$

The posterior probability of the r-th iteration is represented by $\alpha^{(r)}_{ij}$, and the prior probability of the r-th iteration is represented by $\kappa^{(r)}_{ij}$, where the number of iterations is r. It is assumed that the r-th iteration is represented by r; the j-th distribution function is represented by $E(an|\omega(r)j)$. α_{ij} can be obtained by the following formula:

$$\alpha_{ij}^{(t)}=\frac{\kappa_{ij}^{(t)}\sum_{n\in M_i}\frac{O\left(a_n\right)}{T_i}E\left(a_n \mid \omega_j^{(r)}\right)}{\sum_{j=1}^{K}\kappa_{ij}^{(r)}\sum_{n\in M_i}\frac{O\left(a_n\right)}{T_i}E\left(a_n \mid \omega_j^{(r)}\right)} \tag{7}$$

The parameter mean $\lambda^{(r+1)}_j$ and covariance $\sum^{(r+1)}_j$ can be respectively calculated by:

$$\lambda_j^{(r+1)}=\frac{\sum_{i=1}^{M}\sum_{n\in M_i}\alpha_{ij}^{(r)}\frac{O\left(a_n\right)}{T_i}a_n}{\sum_{i=1}^{M}\alpha_{ij}^{(r)}} \tag{8}$$

$$\sum_j^{(r+1)}=\frac{\sum_{i=1}^{M}\sum_{n\in M_i}\alpha_{ij}^{(r)}\frac{O\left(a_n\right)}{T_i}\left(a_n-\lambda_j^{(r)}\right)\left(a_n-\lambda_j^{(r)}\right)^T}{\sum_{i=1}^{M}\alpha_{ij}^{(r)}} \tag{9}$$

Let $\kappa^{(r+1)}_{ij}$ be the prior probability obtained by the region of the i-th pixel. Then, κ_{ij} can be calculated by:

$$\kappa_{ij}^{(r+1)}=\frac{\sum_{n\in M_i}O\left(a_n\right)\alpha_{nj}^{(r)}}{\sum_{j=1}^{K}\sum_{n\in M_i}O\left(a_n\right)\alpha_{nj}^{(r)}} \tag{10}$$

3. MULTI-OBJECTIVE DETECTION

The setting for early childhood education activities targeted at developing children's attentiveness is fairly complicated, and the scene of the activity area image changes quickly. The background changes in the activity space image between the present active video frame and the preceding active video frame can be more accurately detected using the Gaussian mixture model. However, in the collected preschool education activity space image sequences for the development of children's concentration, Gaussian mixture is only appropriate for simple dynamic scenes with few target children, many target children, overlapping colors between the target children and background, or strong light interference. The results of the model's detection will be far less accurate. The speedy detection of many children's targets in the complicated preschool educational environment is a challenge that this research chooses to answer using the ViBe algorithm ViBe+ with complex sceneries (Figure 3).

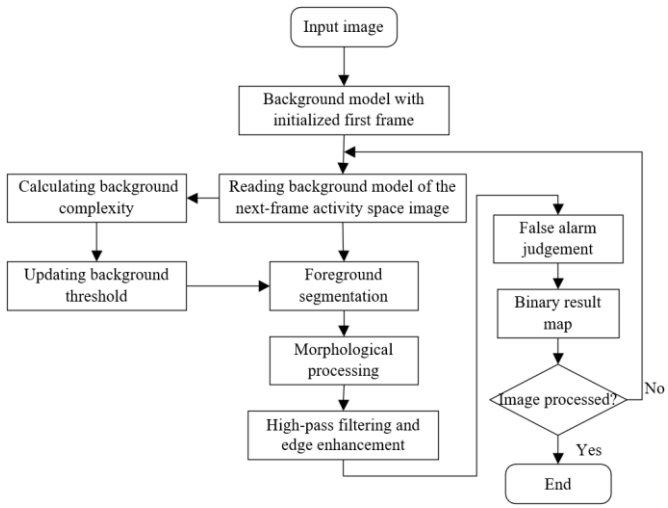

Figure 3. Flow of multitarget detection

The proposed method is divided into three steps: foreground segmentation, target detection post-processing and eliminating false alarm targets. Foreground segmentation aims to characterize the dynamic changes of the current background.

Thus, the background complexity $BF(a)$ corresponding to the target child pixel a to be detected is calculated as follows. Assuming that the position of pixel a in the neighborhood is represented by m, the pixel value of a in the neighborhood is represented by $u(ai)$, and the mathematical expectation in the neighborhood of a is represented by U^*. Then, we have

$$BF(a)=\sqrt{\frac{\sum_{i=1}^{m}\left(u(a_i)-U^*\right)^2}{9}} \tag{11}$$

Then, according to the complexity of the background change of the activity space image, the threshold T used to segment the foreground object and the background of the image is adaptively adjusted based on the following formula, and the initial detection result map of the target child is further obtained. Assume that the global segmentation threshold is denoted by T_0, the global threshold to measure background complexity is denoted by o, and the threshold adjustment parameter is denoted by TZ. Then, threshold T can be configured by:

$$T=\begin{cases}T_0+TZ*\left(BF(a)-o\right), BF(a)\geq o\\ T_0, other\end{cases} \tag{12}$$

The post-processing step of target detection intends to solve the problems of internal holes, noise and edge breaks in the target area. This paper firstly processes the target child's initial detection result map obtained in the foreground segmentation step with mathematical morphology. Let the input preliminary inspection result map be represented by X, and the structural elements be represented by Y. Then, the discrete noise points are eliminated, and the closed operation for filling the internal cavity of the target area can be expressed as:

$$X\cdot Y=\left(X\oplus Y\right)\Theta Y \tag{13}$$

To achieve better smooth suppression of edge noise and highlight the information features of key areas such as contours and edges in the activity space image, this paper chooses the discrete differential Sobel operator combined with Gaussian smoothing and differential derivation, and completes the activity space image edge detection and edge enhancement. Assuming that the convolution template of the Sobel operator in the horizontal direction is represented by O_a, and the convolution template in the vertical direction is represented by O_b. Then, the convolution algorithm implemented by the Sobel operator is as follows:

$$O_b=\begin{bmatrix}-1 & -2 & -1\\ 0 & 0 & 0\\ 1 & 2 & 1\end{bmatrix} \tag{14}$$

$$O_a=\begin{bmatrix}-1 & 0 & 1\\ -2 & 0 & 2\\ -1 & 0 & 1\end{bmatrix} \tag{15}$$

Assume that the horizontal gradient and vertical gradient of the activity space image are represented by $h_a(a,b)$ and $h_b(a,b)$, respectively, the gradient direction is represented by $\omega(a,b)$, and the neighborhood activity space image at the pixel point (a,b) is represented by $g(a+\theta,b+u)$. The related formula can be expressed as:

$$h_a(a,b)=\sum_{q=-1}^{q=1}\sum_{u=-1}^{u=1}O_a(q,u)\,g(a+q,b+u) \tag{16}$$

$$h_b(a,b)=\sum_{q=-1}^{q=1}\sum_{u=-1}^{u=1}O_b(q,u)\,g(a+q,b+u) \tag{17}$$

$$\omega(a,b)=arctan\left(\frac{h_b(a,b)}{h_a(a,b)}\right) \tag{18}$$

To obtain the shape edge features of the target child in the activity space image, this paper constructs an edge feature model corresponding to the foreground area in the original activity space image in the step of eliminating the false alarm target, so as to detect and eliminate the false alarm area of the image. To ensure that the identified target children's shape edges overlap with the actual image shape edges as much as possible, the histogram statistics and normalization processing are performed on $h_a(a,b)$ and $h_b(a,b)$, using the Canny operator. Assume that the number of foreground regions in the activity space image is represented by m, the feature model of the foreground region is represented by E, the vector storing the normalization parameter a_i^* is represented by A, the feature model of the original motion region is represented by W, and the vector storing the normalization parameter is represented by B. Further, the E and W of the feature model can be constructed by:

$$\begin{cases}E_{i(i=1,2,...,m)}=A_i\left(a_{i1},a_{i2},...,a_{i36}\right)\\ W_{i(i=1,2,...,m)}=B_i\left(a_{i1},a_{i2},...,a_{i36}\right)\end{cases} \tag{19}$$

Assuming that the two M-dimensional vectors of the marked edge and the actual edge are represented by A and B respectively, and the value range of a_{ij} and b_{ij} is [0,1]. Then, the feature model similarity $R_i(A_i,B_i)$ can be calculated by:

$$\begin{aligned}R_i(A_i,B_i)&=\frac{A\cap B}{A\cup B}=\frac{A_i\bullet B_i}{\|A_i\|^2+\|B_i\|^2-A_i\bullet B_i}\\ &=\frac{\sum_{j=1}^{M}a_{ij}b_{ij}}{\sqrt{\sum_{j=1}^{M}\left(a_{ij}\right)^2+\sum_{j=1}^{M}\left(b_{ij}\right)^2\sum_{j=1}^{M}a_{ij}b_{ij}}}\end{aligned} \tag{20}$$

It can be seen from the above formula that when A and B are non-zero vectors, and $A_i=B_i$, $R_i(A_i,B_i)=1$, according to the following formula, $R_i(A_i,B_i)<1$ when $A_i\neq B_i$. If one of Ai and Bi is a zero vector, then $R_i(A_i,B_i)=0$.

$$R_i(A_i,B_i)\leq\frac{\sum_{j=1}^{M}a_{ij}\cdot b_{ij}}{2\sum_{j=1}^{M}a_{ij}b_{ij}-\sum_{j=1}^{M}a_{ij}b_{ij}}=1 \tag{21}$$

False alarm target elimination: The degree of similarity between the foreground area characteristics of the extracted activity space image and the equivalent activity space area features of the original image can be determined when the similarity judgment of vectors A and B is complete. The

similarity between determinable quantity features increases as $R_i(A_i,B_i)$ approaches 1. It is determined that the foreground area is not a false alarm area when $R_i(A_i,B_i)$ is less than the similarity threshold T_0, and all of the pixels' values in the foreground area are left alone. Otherwise, set all of the area's pixel values to zero. The technique for removing false alarm targets is depicted in Figure 4.

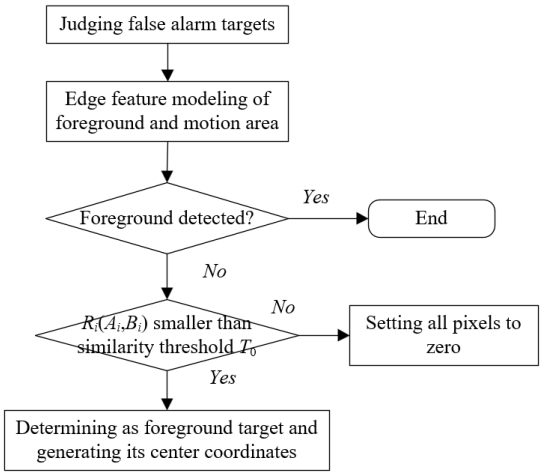

Figure 4. Flow of false alarm target elimination

4. EXPERIMENTS AND RESULTS ANALYSIS

Follow the implementation plan of the children's home for preschool education activities, preschool education activity interventions were carried out in different sports forms 4 times a week for 6 weeks (1 time on Monday, 2 times on Tuesday, 1 time on Wednesday, 2 times on Thursday, and 1 time on Friday). The specific preschool education activity intervention plan is shown in Table 1.

Table 2 compares the image processing accuracy for different child targets. It can be seen that in practical applications, the improved Gaussian mixture model GMM+ for ordinary activity scenes and the improved ViBe algorithm ViBe+ for complex activity scenes perform better in both subjective vision and objective evaluation indices. Compared with the frame difference method and background difference method, the image segmentation and target detection results of the proposed algorithm are highly accurate and robust.

Our algorithm effectively eliminates the false alarm area. To verify the superiority of our algorithm, frame difference method, background difference method, our GMM+, and our ViBe+ are designed based on the 7-frame continuous images in the video image sequence of preschool education activities. Figure 5 compares the performance of the four algorithms. It can be seen that our algorithms perform significantly better than the frame difference method and background difference method in different activity scenarios, which verifies the effectiveness and applicability of the GMM+ and ViBe+.

To further disclose the development features of children of different ages in preschool education activities, this paper performs frequency counting and significance testing of the concentration behaviors of bottom, middle, and top class children in the preschool education activity scenarios, which are identified by the proposed image processing method.

Table 1. Intervention plans

Activity	Content	Duration	Load	Intervention cycle	Intervention frequency
Group dance	A Girl Picking up Mushrooms×2	≧10min			
Cheerleading	Children's Cheerleading×2	≧12min	Moderate	6 weeks	7 times/ week
Arching	8*vs*8 half court confrontation	≧20min			

Table 2. Comparison of image processing accuracies

		frame difference method	background difference method	*Our GMM+*	Our *ViBe+*
Target 1	*PA*	0.5281	0.7485	0.7958	0.9581
	Dice	0.5741	0.5782	0.5908	0.6739
		frame difference method	background difference method	*GMM+*	*ViBe+*
Target 2	*PA*	0.6135	0.8631	0.8547	0.8526
	Dice	0.6489	0.7152	0.7282	0.7629
		frame difference method	background difference method	*GMM+*	*ViBe+*
Target 3	*PA*	0.6392	0.6938	0.7847	0.7429
	Dice	0.5367	0.5612	0.5478	0.6958
		frame difference method	background difference method	*GMM+*	*ViBe+*
Target 4	*PA*	0.6415	0.8586	0.7695	0.9142
	Dice	0.6748	0.8475	0.6241	0.9485

Table 3. Frequency of concentration behaviors of children of different ages

Variable	Age						Total
	Bottom class	Percentage	Middle class	Percentage	Top class	Percentage	
Attentive	51	22.36%	69	36.29%	71	31.25%	185
Focused	47	24.81%	61	30.41%	76	39.47%	162
Serious	92	20.39%	183	35.27%	229	41.29%	415
Anti-interference	27	28.41%	39	39.26%	41	48.72%	174
Listening	90	41.26%	65	34.49%	56	21.36%	261

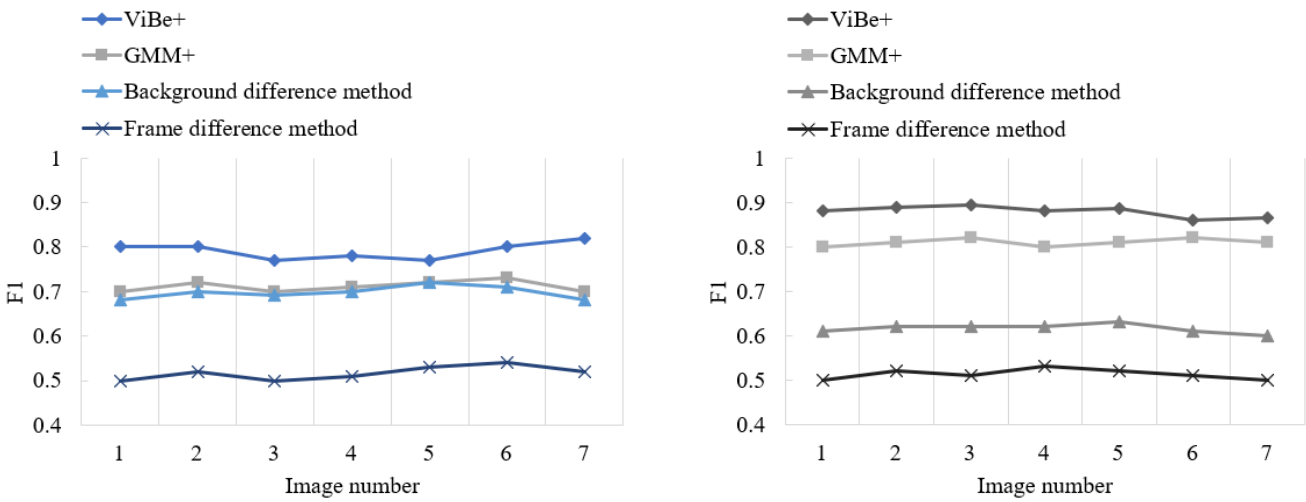

Figure 5. Performance comparison of the four algorithms

Table 4. Chi-squared test results

Variables	X^2	*df*	*sig*
Attentive	6.258	3	0.052*
Focused	7.162	3	0.069***
Serious	36.295	3	0.024*
Anti-interference	6.581	3	0.062**
Listening	15.347	3	0.085***

The relevant experimental results are shown in Tables 3 and 4. It can be seen that the children reached the significant levels on the five concentration behaviors, including attentive, focusing, serious, anti-interference, and listening. In the background of preschool education activities, the children's thinking gradually increases with concentration behaviors, as they get older and older.

Table 5. Descriptive statistics on concentration behaviors at different levels of intervention

Intervention level	Attentive	Focused	(Standard deviation/mean) Serious	Anti-interference	Listening
I	0.958/3.529	16.351/52.619	7.629/4.301	1.639/0.427	9.328/24.518
II	1.274/3.614	10.251/62.352	3.958/4.749	0.528/0.531	13.526/27.485
III	2.925/3.747	17.241/74.367	7.621/5.628	0.596/0.516	12.528/29.634
IV	1.928/3.728	19.628/73.582	7.514/5.693	0.345/0.662	15.284/28.306
V	1.037/3.925	8.954/78.265	3.258/4.247	1.528/0.627	8.625/23.614
VI	1.847/3.128	9.107/65.637	3.695/1.204	0.629/0.391	8.297/15.378

Table 5 presents the descriptive statistics of each concentration behavior under different intervention levels. It can be seen that under the intervention levels of preschool education activities, which are ranked from high to low, the mean values of the five concentration behaviors are mostly close, but the 5 concentration behaviors under the two middle intervention levels of III and IV are relatively close. The scores of the five attention behaviors were higher, and the scores of the five attention behaviors were lower under excessively high or low intervention. It has been verified that the intervention intensity of appropriate preschool education activities will help children improve their concentration.

5. CONCLUSIONS

In order to cultivate children's attentiveness, this study performs research on image segmentation and target extraction of activity space in preschool education. Preschool educational activity intervention and children's concentration are related, and the frequency-tuned saliency algorithm is added to the created Gaussian mixture model to realize the construction of spatial information of preschool educational activity space images for the development of children's concentration and Activity space image segmentation. The ViBe algorithm with complex scenes ViBe+ is chosen to realize the rapid detection of multiple child targets in complex preschool educational activity environments. This algorithm targets issues like small target children, large numbers of target children, color overlap between the target children and the background, or strong light interference.

The intervention plans for different preschool education activities were formulated through experiments. The image processing accuracies on different children targets were compared. It was found that our algorithm achieved more accurate and robust effect in image segmentation and target detection than frame difference method and background difference method. In addition, this paper performs frequency counting and significance testing of the concentration behaviors of bottom, middle, and top class children in the preschool education activity scenarios, and further discloses the development features of children of different ages in preschool education activities.

ACKNOWLEDGEMENT

This paper was supported by Scientific Research Foundation for Henan Finance University (Grant No.: 2021BS010).

REFERENCES

[1] Dan, G., Ruxandra, M.O., Claudiu, D., et al. (2022). Gaze analysis and concentration monitoring for children with attention disorder using eye-tracking. In 2022 IEEE International Conference on Automation, Quality and Testing, Robotics (AQTR), Cluj-Napoca, Romania, pp. 1-6. https://doi.org/10.1109/AQTR55203.2022.9802014

[2] Jyoti, V., Lahiri, U. (2022). Portable joint attention skill training platform for children with autism. IEEE Transactions on Learning Technologies, 15(2): 290-300. https://doi.org/10.1109/TLT.2022.3169964

[3] Duan, G., Han, Q., Yao, M., Li, R. (2022). Effects of rhythmic gymnastics on joint attention and emotional problems of autistic children: A preliminary investigation. Computational Intelligence and Neuroscience, 2022: 2596095. https://doi.org/10.1155/2022/2596095

[4] Xing, J., Zhang, Y., Xu, S., Zeng, X. (2022). Nanomaterial assisted diagnosis of dopamine to determine attention deficit hyperactivity disorder-'an issue with Chinese children'. Process Biochemistry, 118: 112-120. https://doi.org/10.1016/j.procbio.2022.01.012

[5] Mealings, K. (2022). Classroom acoustics and cognition: A review of the effects of noise and reverberation on primary school children's attention and memory. Building Acoustics, 29(3): 401-431. https://doi.org/10.1177/1351010X221104892

[6] Liu, S., Mao, S. (2022). An intervention study on children's healthy joint attention skills based on a mixed instructional approach of DTT and PRT. Journal of Healthcare Engineering, 2022: 5987582. https://doi.org/10.1155/2022/5987582

[7] Banire, B., Al Thani, D., Qaraqe, M., Mansoor, B., Makki, M. (2021). Impact of mainstream classroom setting on attention of children with autism spectrum disorder: An eye-tracking study. Universal Access in the Information Society, 20(4): 785-795. https://doi.org/10.1007/s10209-020-00749-0

[8] Jiang, K., Wang, Y., Feng, Z., Sze, N.N., Yu, Z., Cui, J. (2021). Exploring the crossing behaviours and visual attention allocation of children in primary school in an outdoor road environment. Cognition, Technology & Work, 23(3): 587-604. https://doi.org/10.1007/s10111-020-00640-1

[9] Lauricella, A.R., Aladé, F., Russo, M., Strevett, A., Herdzina, J. (2022). Children's visual attention and comprehension from synchronous video book reading. Computers & Education, 191: 104628. https://doi.org/10.1016/j.compedu.2022.104628

[10] Sun, W. (2022). Design of auxiliary teaching system for preschool education specialty courses based on artificial intelligence. Mathematical Problems in Engineering, 2022: 4504707. https://doi.org/10.1155/2022/4504707

[11] Chen, X., Jin, G. (2022). Preschool education interactive system based on smart sensor image recognition. Wireless Communications and Mobile Computing, 2022: 2556808. https://doi.org/10.1155/2022/2556808

[12] Li, S. (2022). Preschool education students' understanding of children's picture books. Wireless Communications and Mobile Computing, 2022: 9697874. https://doi.org/10.1155/2022/9697874

[13] Wang, X. (2022). Optimization of child literature curriculum settings for preschool education based on numerical analysis. Mathematical Problems in Engineering, 2022: 8452166. https://doi.org/10.1155/2022/8452166

[14] Wang, Z., Dong, W. (2022). Statistically based assessment and decision-making in preschool education. Mathematical Problems in Engineering, 2022: 7447246. https://doi.org/10.1155/2022/7447246

[15] Li, X. (2022). Deep-learning-guided student classroom action understanding for preschool education. Applied Bionics and Biomechanics, 2022: 9416467. https://doi.org/10.1155/2022/9416467

[16] Li, X., Xiao, W. (2022). Application of wireless network based on artificial intelligence in network teaching of preschool education manual and aesthetic education practical course. Mathematical Problems in Engineering, 2022: 6729830. https://doi.org/10.1155/2022/6729830

[17] Gao, H., Liu, L. (2020). Construction of school-enterprise cooperation training platform for preschool education in the "Internet+" era. In Innovative Computing, pp. 245-250. https://doi.org/10.1007/978-981-15-5959-4_30

[18] Quispe Lloccallasi, R., Saul Huaynacho Peñaloza, A. (2020). Application of attendance control and learning activities using WhatsAPP for preschool education. In 2020 The 4th International Conference on Education and E-Learning, Yamanashi, Japan, pp, pp. 23-26. https://doi.org/10.1145/3439147.3439173

[19] Yu, L., Luo, F. (2022). Research on children's attention score modeling based on facial micro expression feature. In 2022 IEEE 5th Eurasian Conference on Educational Innovation (ECEI), Taipei, Taiwan, pp. 241-244. https://doi.org/10.1109/ECEI53102.2022.9829516

[20] Kokkalia, G., Drigas, A., Economou, A. (2016). The role of games in special preschool education. International Journal of Emerging Technologies in Learning, 11(12): 30-35. https://doi.org/10.3991/ijet.v11i12.5945

[21] Hosseini, A., Fazeli, S., van Vliet, E., Valencia, L., Habre, R., Sarrafzadeh, M., Bui, A. (2018, July). Children activity recognition: Challenges and strategies. In 2018 40th Annual International Conference of the IEEE Engineering in Medicine and Biology Society (EMBC), Honolulu, HI, USA, pp. 4331-4334. https://doi.org/10.1109/EMBC.2018.8513320

[22] Basak, P., De, S., Agarwal, M., Malhotra, A., Vatsa, M., Singh, R. (2017). Multimodal biometric recognition for toddlers and pre-school children. In 2017 IEEE International Joint Conference on Biometrics (IJCB), Denver, CO, USA, pp. 627-633. https://doi.org/10.1109/BTAS.2017.8272750